Fabrication and Analysis of Epitaxially Grown $Ge_{1-x}Sn_x$ Microdisk Resonator With 20-nm Free-Spectral Range

Seongjae Cho, *Member, IEEE*, Robert Chen, Sukmo Koo, Gary Shambat, Hai Lin, Namkyoo Park, *Member, IEEE*, Jelena Vučković, *Member, IEEE*, Theodore I. Kamins, *Fellow, IEEE*, Byung-Gook Park, *Member, IEEE*, and James S. Harris, Jr., *Fellow, IEEE*

***Abstract*—In this work, a whispering gallery mode (WGM) microdisk resonator based on $Ge_{1-x}Sn_x$ grown by molecular beam epitaxy (MBE) was fabricated and characterized. Various process conditions and different Sn contents (4% and 1%) were explored to confirm the feasibility of $Ge_{1-x}Sn_x$ for microcavity device operation. Optical modes with wavelengths in the infrared (IR) range beyond 1550 nm were successfully confined in the devices fabricated with different diameters, and free-spectral ranges (FSRs) near 20 nm were obtained.**

***Index Terms*—Free-spectral range (FSR), GeSn, infrared (IR), microdisk resonator, molecular beam epitaxy (MBE), whispering gallery mode (WGM).**

I. Introduction

WHISPERING gallery mode (WGM) microdisk resonators are widely used for conventional dielectric resonators in advanced radio frequency (RF) circuits, optical communication systems, and biosensing devices because of their simple device structure, high quality factor, and the possibility of both transverse electric (TE) and transverse magnetic (TM) mode operations [1]–[3]. There has been intensive research on novel materials and processes for the integration of advanced optoelectronic and photonic systems on silicon because of silicon's cost-effectiveness and compatibility with complementary metal-oxide-semiconductor (CMOS) circuits [4]. To ease integration with silicon electronics, group IV species and their alloys are attracting great attention as good candidates for the active material [5]. $Ge_{1-x}Sn_x$ is considered to be an attractive material for optical and electronic devices [6], [7] due to its Γ and L-valley energy bandgap tunability by varying the Sn content (to possibly obtain a direct bandgap), growth on silicon via appropriate buffer layers, and high carrier mobility. In this work, WGM microdisk resonators based on $Ge_{1-x}Sn_x$ grown by molecular beam epitaxy (MBE) were successfully fabricated, and their absorption characteristics were investigated for the first time. Different Sn contents ($x = 0.04$ and 0.01) were explored, and the Γ-valley energy bandgaps in both cases were decreased to less than that of pure Ge (0.8 eV), corresponding to wavelengths greater than 1550 nm. Thus, the GeSn microdisk resonator is suitable for infrared (IR) signal processing. Several significant advantages are expected for a $Ge_{1-x}Sn_x$-based microdisk resonator: (1) With a possible direct bandgap, highly efficient laser or luminescent devices can be obtained without the need to provide momentum to allow electron-hole recombination. (2) The smaller bandgap energy enables the WGM resonator to operate in the short-wavelength IR regime, which is not possible using either Si or Ge. (3) The higher refractive index obtained by introducing Sn results in a reliable free-spectral range (FSR). For devices with $Ge_{0.99}Sn_{0.01}$ grown at a low temperature, FSRs near 20 nm were obtained.

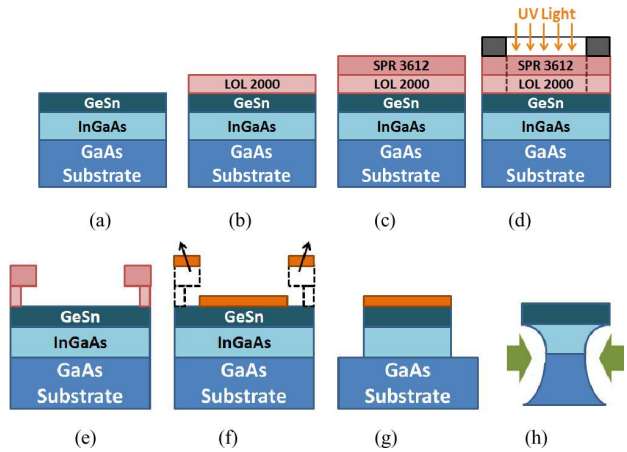

Fig. 1. Process integration for GeSn WGM microdisk resonator using Cr liftoff patterning technique. (a) InGaAs buffer and GeSn growth by MBE. (b) First and (c) second liftoff PR deposition. (d) Photolithography. (e) Develop and first PR layer undercut. (f) Cr liftoff. (g) Dry etch. (h) GaAs wet etch and Cr removal.

II. Device Fabrication

Fig. 1 illustrates the process used to fabricate the GeSn microdisk resonators. A GeSn layer was first grown on a GaAs substrate by MBE. (For this initial investigation, a GaAs substrate was used to demonstrate the behavior of the resonator without

Manuscript received April 01, 2011; revised July 13, 2011; accepted July 26, 2011. Date of publication August 08, 2011; date of current version September 28, 2011. This work was supported in part by the SRC Interconnect Focus Center Research Program and in part by the U.S. Government through Advanced Photonic Integrated Circuits (APIC). The work of R. Chen was supported by a National Science Foundation (NSF) Graduate Fellowship. The work of H. Lin was supported by a Stanford Graduate Fellowship.

S. Cho, R. Chen, G. Shambat, H. Lin, J. Vučković, T. I. Kamins, B.-G. Park, and J. S. Harris, Jr. are with the Department of Electrical Engineering, Stanford University, CA 94305-4075 USA (e-mail: felixcho@stanford.edu; robert.chen@stanford.edu; gshambat@gmail.com; hailin@stanford.edu; jela@stanford.edu; kamins@stanford.edu; bgpark@snu.ac.kr; harris@snow.stanford.edu).

S. Koo and N. Park are with the School of Electrical Engineering and Computer Science, Seoul National University, Seoul 151-742, Korea (e-mail: odengmo@gmail.com; nkpark@gmail.com).

Color versions of one or more of the figures in this letter are available online at http://ieeexplore.ieee.org.

Digital Object Identifier 10.1109/LPT.2011.2163929

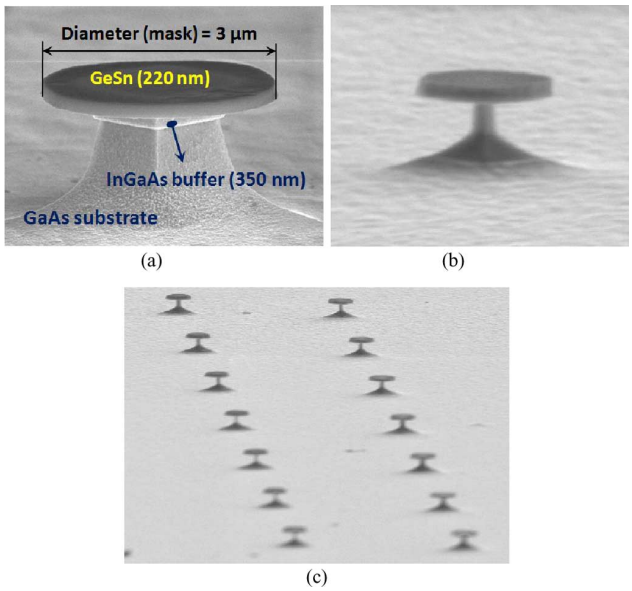

Fig. 2. SEM images of the fabricated $Ge_{1-x}Sn_x$ devices. (a) $x = 0.04$, thickness $(T) = 220$ nm and $D = 3$ μm. (b) $x = 0.01$, $T = 260$ nm, and $D = 2$ μm (D's were 2–10 μm). (c) Microdisk array.

complications of the lattice-mismatched substrate and relaxed buffer layer that would be used on a Si substrate.) For some devices, an InGaAs buffer layer was used, without exposure to air between depositions. The GeSn was defined using either a Cr liftoff process or conventional photoresist. The liftoff process is illustrated in Fig. 1(b)–(f).

The GeSn was then dry etched and the GaAs substrate was chemically etched by a H_2O:H_2O_2:$H_2SO_4 = 8$:1:1 solution for 20 s at room temperature without stirring. The etch composition was carefully controlled to etch 800 nm laterally from the GeSn outer perimeter, leaving a supporting GaAs pillar even for devices with the smallest diameter of 2 μm. This undercut etch process provides effective confinement of the optical modes to the disk perimeter and minimizes coupling to the substrate. To be compatible with the diameter of the optical fiber used in the measurements, the dry etch process removed more than 500 nm of the GaAs substrate, as well as the GeSn layer, to provide adequate offset from the final GaAs substrate. Devices with diameters larger than 3 μm were fabricated using photoresist as an etch mask, rather than the liftoff process. The final distance between device and substrate was 1.5 μm, which eliminated any difficulty in coupling the optical fiber to the WGM microdisk resonator. Fig. 2 shows scanning electron microscope (SEM) images of fabricated WGM microdisk resonators and an array.

III. Measurement Results

Fig. 3(a) shows a schematic view of the optical transmission measurement setup developed by G. Shambat *et al.* [8]. An Agilent 83437A broadband light source (BLS) and an Agilent 86140B optical spectrum analyzer (OSA) were used to generate and detect the IR light. Light was transmitted through an optical fiber tapered to a diameter of 1 μm in contact with the fabricated devices. Fig. 3(b) shows an optical microscope image of the sample. The distances between devices were larger than 20 μm so that no unwanted signal from adjacent devices would be coupled. Fig. 4(a) and (b) show measured results from a $Ge_{0.96}Sn_{0.04}$ device with $D = 3$ μm and a $Ge_{0.99}Sn_{0.01}$ device

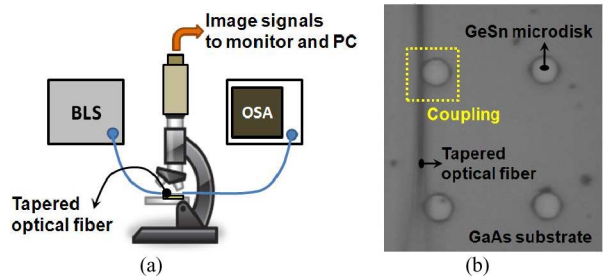

Fig. 3. Optical measurement setup. (a) Schematic view of the setup. (b) Optical microscope image. The upper limits in wavelengths of broadband light source (BLS) and optical spectrum analyzer (OSA) were 1700 nm.

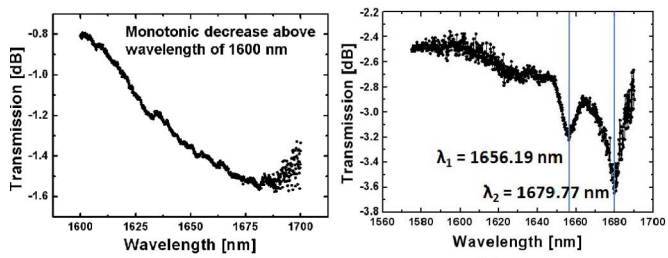

Fig. 4. Measured optical transmission characteristics. (a) $Ge_{0.96}Sn_{0.04}$ ($T = 220$ nm and $D = 3$ μm) and (b) $Ge_{0.99}Sn_{0.01}$ microdisks ($T = 260$ nm and $D = 2$ μm).

with $D = 2$ μm, respectively. A monotonic decrease in transmission starts at wavelengths slightly shorter than 1600 nm in both cases, consistent with the energy bandgap of the Γ-valley decreasing when Sn atoms are introduced [9]. Light with wavelengths longer than 1550 nm, which corresponds to the Γ-bandgap energy of pure Ge (0.8 eV), is effectively coupled and confined by the devices. For the $Ge_{0.99}Sn_{0.01}$ device two optical modes were observed at $\lambda_1 = 1656.19$ nm and $\lambda_2 = 1679.77$ nm; for the $Ge_{0.96}Sn_{0.04}$ device, the optical modes were obscured by the bandgap edge. The effective refractive indices (n_{eff}) at λ_1 and λ_2 were 3.430 and 3.403, respectively, and an effective diameter (D_{eff}) of 1.95 μm (2.5% reduction) was obtained by recursion. This behavior shows that optical modes were well confined. The coupling loss is reduced as the coupling distance increases to 500 nm [8]. However, the optical fiber was manually positioned to make contact with the device, which introduces a significant coupling loss. The material losses were reduced by passivating the side surfaces of the $Ge_{0.99}Sn_{0.01}$ devices by annealing in forming gas at 550 for 30 s, as seen by comparing Fig. 4(a) and (b). Based on finite-difference time-domain (FDTD) simulations, devices $(D = 3$ μm) with 4 evenly spaced nanoholes (simulating surface roughness), of radii 50 nm and 200 nm, showed degradation of the quality factor by 47% and 83%, respectively, compared with a device having no nanohole.

Fig. 5(a) plots the measured n values of $Ge_{0.99}Sn_{0.01}$ for wavelengths from 1550 nm to 1688 nm, which can be linearly fitted as

$$n = 5.15192 - 6.06447 \times 10^{-4}\lambda \tag{1}$$

where λ has the units of nm. The FSR is defined by the relation

$$\Delta\lambda_{FSR} = \frac{n_{eff}(\lambda_l)L}{m} - \frac{n_{eff}(\lambda_{l-1})L}{m+1},$$
$$L = 2\pi R_{eff} = \pi D_{eff},$$

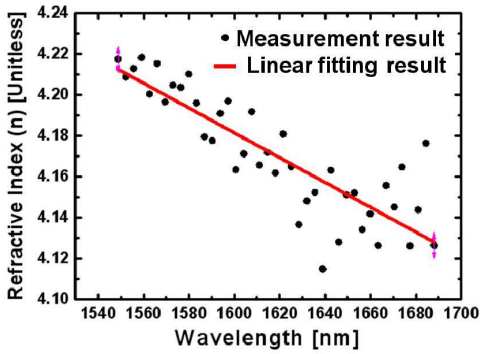

(a)

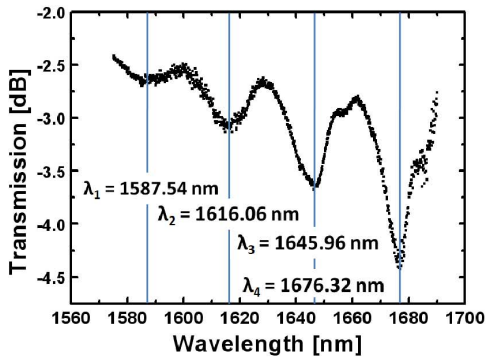

(b)

Fig. 5. Measurement results. (a) Refractive index of $Ge_{0.99}Sn_{0.01}$. (b) Optical transmission of a $Ge_{0.99}Sn_{0.01}$ microdisk resonator with $D = 8\ \mu$m.

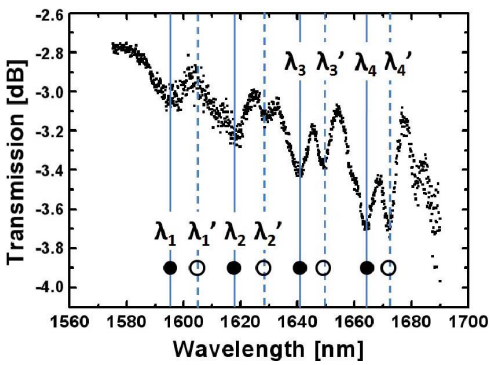

Fig. 6. Measured absorption curve of a $Ge_{0.99}Sn_{0.01}$ device ($D = 10\ \mu$m).

$$n_{eff}{}^2 = n_g{}^2 b + n_c{}^2(1-b), b \sim 1 - \frac{\ln(1+\frac{V^2}{2})}{\frac{V^2}{2}},$$
$$V = \frac{2\pi}{\lambda} \times d\sqrt{n_g{}^2 - n_c{}^2}. \quad (2)$$

where λ_l is the next longer resonant wavelength than λ_{l-1}, n_g and n_c are refractive indices of guiding and cladding materials (which are $Ge_{0.99}Sn_{0.01}$ and air, respectively), b is the field confinement factor, V is the normalized frequency [10], and d is the disk thickness. A set of three second-order equations with $l = 2$, 3, and 4 were set up, from which three m values were extracted. From recursive calculations for a resonator with $D = 8\ \mu$m, $D_{\text{eff}} = 7.6\ \mu$m (5% reduction) and $m(\lambda_1) = 44$, $m(\lambda_2) = 43$, $m(\lambda_3) = 42$, and $m(\lambda_4) = 41$ [Fig. 5(b)]. Fig. 6 shows the transmission curve of a device with $D = 10\ \mu$m. As in the previous cases, the bandgap edge is determined to be around 1580 nm. The paired dips are from TE and TM modes (filled and open circles, respectively), which can be determined by comparing the wavelengths in each doublet [11]. The extracted m values of the measured modes were $m(\lambda_1 = 1595.16\text{ nm}) = 56$, $m(\lambda_2 = 1617.55\text{ nm}) = 55$, $m(\lambda_3 = 1640.55\text{ nm}) = 54$, and $m(\lambda_4 = 1664.13\text{ nm}) = 53$ with $D_{\text{eff}} = 9.7\ \mu$m (3% reduction). The measured FSR's are nearly 20 nm, which is large enough to avoid misreading a newly visible mode at λ_i' as an existing one at λ_{i+1}.

$$|\lambda_i' - \lambda_i| \quad (\text{Sensing Margin}) = |\lambda_{i+1} - \lambda_i'| < \text{FSR}, \quad i = 1, 2, 3, 4. \quad (3)$$

From the FDTD simulation results, the temperature sensitivity of a $Ge_{0.99}Sn_{0.01}$ microdisk resonator ($D = 10\ \mu$m) was 0.29 nm/K, which is 3 times as high as that of a pure Si device (0.09 nm/K) at 295 K. The cavity modes should redshift due to the increase in refractive index caused by the bandgap reduction [9].

IV. Conclusion

WGM microdisk resonators of MBE-grown GeSn (4% and 1% Sn) have been successfully fabricated and characterized. The fabricated devices confined multiple optical modes from the bandgap edge up to 1700 nm and showed 20-nm FSR, which is larger than the wavelength difference $\Delta\lambda$ between TE and TM modes. Due to their process compatibility and reliable operation, GeSn microdisk resonators can be a core element in Si CMOS-integrated photonic circuits.

References

[1] M. E. Tobar, E. N. Ivanov, P. Blondy, D. Cros, and P. Guillon, "High-Q whispering gallery travelling wave resonators for oscillator frequency stabilization," *IEEE Trans. Ultrason., Ferroelectr., Freq. Control*, vol. 47, no. 2, pp. 421–426, Mar. 2000.

[2] B. Min, E. Ostby, V. Sorger, E. U-Avila, L. Yang, X. Zhang, and K. Vahala, "High-Q surface-plasmon-polariton whispering-gallery microcavity," *Nature*, vol. 457, pp. 455–458, Jan. 2009.

[3] S. Arnold, D. Keng, S. I. Shopova, S. Holler, W. Zurawsky, and F. Vollmer, "Whispering gallery mode carousel—A photonic mechanism for enhanced nanoparticle detection in biosensing," *Opt. Express*, vol. 17, no. 8, pp. 6230–6238, Apr. 2009.

[4] D. Choi, E. Kim, P. C. McIntyre, and J. S. Harris, "Molecular-beam epitaxial growth of III–V semiconductors on Ge/Si for metal-oxide-semiconductor device fabrication," *Appl. Phys. Lett.*, vol. 92, no. 20, pp. 203502–203502, May 2008.

[5] J. Kolodzey, P. R. Berger, B. A. Orner, D. Hits, F. Chen, A. Khan, X. Shao, M. M. Waite, S. I. Shah, C. P. Swann, and K. M. Unruh, "Optical and electronic properties of SiGeC alloys grown on Si substrates," *J. Cryst. Growth*, vol. 157, no. 1–4, pp. 386–391, Dec. 1995.

[6] H. P. L. Guevara, A. G. Rodríguez, H. Navarro-Contreras, and M. A. Vidal, "Determination of the optical energy gap of $Ge_{1-x}Sn_x$ alloys with $0 < x < 0.14$," *Appl. Phys. Lett.*, vol. 84, no. 22, pp. 4532–4534, May 2004.

[7] O. Nakatsuka, N. Tsutsui, Y. Shimura, S. Takeuchi, A. Sakai, and S. Zaima, "Mobility behavior of $Ge_{1-x}Sn_x$ layers grown on silicon-on-Insulator substrates," *Jpn. J. Appl. Phys.*, vol. 49, no. 4, pp. 04DA10–04DA10, Apr. 2010.

[8] G. Shambat, Y. Gong, J. Lu, S. Yerci, R. Li, L. D. Negro, and J. Vučković, "Coupled fiber taper extraction of 1.53 μm photoluminescence from erbium doped silicon nitride photonic crystal cavaties," *Opt. Express*, vol. 18, no. 6, pp. 5964–5973, Mar. 2010.

[9] G. Shambat, S.-L. Cheng, J. Lu, Y. Nishi, and J. Vuckovic, "Direct band Ge photoluminescence near 1.6 μm coupled to Ge-on-Si microdisk resonators," *Appl. Phys. Lett.*, vol. 97, no. 24, pp. 241102–241102, Dec. 2010.

[10] J. Vuckovic, *Introduction to Nanophotonics and Nanostructures at Stanford University*. Stanford: Stanford Univ., 2010, ch. 2, pp. 30–35.

[11] J. Krupka, D. Cros, M. Aubourg, and P. Guillon, "Study of whispering gallery modes in anisotropic single-crystal dielectric resonators," *IEEE Trans. Microw. Theory Tech.*, vol. 42, no. 1, pp. 56–61, Jan. 1994.